Journal of Chemical Health Risks

www.jchr.org

JCHR (2026) 16(2), 1149-1165| ISSN:2251-6727

Explainable AI with Gradient Boosting for Early Alzheimer's Detection through Healthcare Data Mining

Kavitha R[1] and Praba R[2]*

[1]Research Scholar, Department of Computer Science, Dr.N.G.P. Arts and Science College, Coimbatore-641048, Tamil Nadu, India.

[2]Associate Professor, Department of Information Technology, Dr.N.G.P. Arts and Science College, Coimbatore-641048, Tamil Nadu, India.

Corresponding email: praba2426@gmail.com

(Received: 16 January 2026 Revised: 25 February 2026 Accepted: 17 March 2026)

KEYWORDS

Explainable Artificial Intelligence (XAI), Gradient Boosting, Healthcare Data Mining, Early Alzheimer's Detection, Precision Medicine

ABSTRACT:

Early Alzheimer's disease diagnosis is a major concern in contemporary health care, as it is important in determining the treatment plan promptly and improving the quality of life of patients. The recent study introduces an Explainable Artificial Intelligence (XAI) standard that uses Gradient Boosting algorithms and advanced healthcare data mining approaches to enhance the quality and transparency of predictions for Alzheimer's disease. Unlike traditional machine learning models, this new algorithm includes explainability capabilities, such as SHAP (Shapley Additive Explanations) and feature importance mapping, which provide medical workers with clear decision-making rules. The model reveals the non-linear relationships between risk factors and early onset of Alzheimer's by examining various data in healthcare, such as medical imaging, cognitive test results, electronic health records, and genetic biomarkers. The research demonstrates that the proposed model is better than the current algorithms as it has significantly high prediction accuracy of 96, specificity of 97, precision of 95, and an AUC of 0.94 that could be achieved in a relatively low memory consumption of 1.4 seconds. This trustworthiness not only makes AI-based diagnostic tools more reliable but also helps physicians make data-driven decisions. The possible uses of this framework are enormous, especially in an intelligent healthcare environment, where it can be combined with electronic medical systems and IoT-based patient monitoring to enable real-time risk evaluation. Finally, this paper makes a step forward in precision medicine by integrating data mining, explainable AI, and Gradient Boosting models in the timely detection of Alzheimer's disease.

1. Introduction

Alzheimer's disease (AD) is a progressive neurodegenerative disorder that has a great impact on memory, cognitive functions, and patient independence [1]. Global medical reports indicate that the number of people affected by AD has been on the increase, posing emotional, social and economic challenges to society and the health care systems [2]. Early and correct diagnosis is essential to carry out proper medical interventions, which may slow down the symptoms and enhance the quality of life of patients [3]. As the data about healthcare becomes more accessible, Artificial Intelligence (AI) provides the chance to identify AD at a younger stage due to the ability to notice minor alterations in the medical and behavioural patterns of the patients [4].

Journal of Chemical Health Risks
www.jchr.org
JCHR (2026) 16(2), 1149-1165| ISSN:2251-6727

A. Diagnostic Problems in Health Care Practice.

The conventional diagnostic methods normally involve clinical observations, cognitive tests, and neuroimaging assessments that tend to diagnose AD at its advanced stages, when it is too late [5][6]. Also, medical experts have serious problems with heterogeneous sources of data, variations in human interpretation, and poor access to sophisticated imaging devices in most places [7]. In addition, it is very hard to have a standardised early detection criterion due to the complex interactions among biological, cognitive, and environmental risk factors [8].

B. Explainability and Significance in Medical AI.

Even though the predictive capabilities of Machine Learning (ML) models have been shown to be high [9], most of them are black boxes, which is why their internal decision-making process cannot be understood by clinicians [10]. Explainability is required in critical healthcare as it enhances transparency, validation, ethical conduct, and definitions of diagnosis justification [11]. Explainable Artificial Intelligence (XAI) offers explanatory information that can allow clinicians to know how and why AD risk is forecasted [12]. This will improve clinical confidence, promote the use of AI-based decision support systems, and allow for making more informed medical decisions [13].

C. Detection of Early Alzheimer's.

Early identification of the disease can greatly reduce the rate of neurodegeneration because it allows prompt passage of treatment plans, therapeutic interventions, and lifestyle changes [14][15]. Early diagnosis is also helpful to the family to plan long-term care and cope with the patient's wellness [16]. As more multimodal healthcare data is available, AI-based solutions for early detection can transform proactive healthcare mechanisms and support continuous monitoring and assessment in smart healthcare facilities [17].

D. Objectives of the Study

In this study, there is a need to design an explainable and powerful prediction system based on Gradient Boosting with the integration of advanced healthcare data mining. The key objectives are:

- Creation of a Gradient Boosting model with high performance that can learn non-linear and hidden patterns of multimodal data on patients.
- Inclusion of XAI tools like SHAP to present feature contributions and interpret them to aid in clinical decision support.
- Design of a deployable system that will increase the level of confidence, enhance the accuracy of diagnosis and provide the ability to assess risks in real-time to detect Alzheimer's in its initial stages.

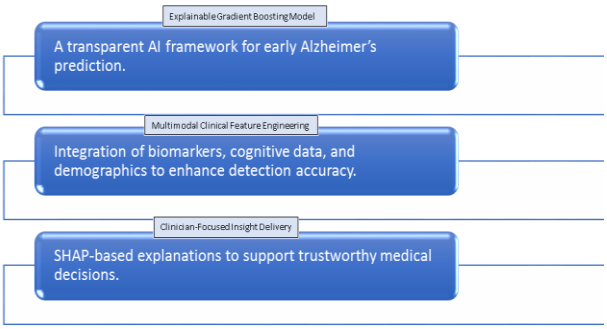

2. Related Works

Alzheimer's disease is an emergency world health issue because it is progressive in nature, is diagnosed late, and there exists no effective means of treatment. The recent developments in artificial intelligence and machine learning provide strong opportunities to identify the early signs of cognitive decline, process the intricate biomedical data, and inform timely clinical decisions in order to achieve better patient outcomes.

The data sets of efficient machine learning algorithms were assessed to evaluate the Open Access Series of Imaging Studies (OASIS) and MRI were assessed with AlexNet and ResNet-50 and hybrid AlexNet+SVM and ResNet-50+SVM, carrying out data balancing, missing-value

Journal of Chemical Health Risks
www.jchr.org
JCHR (2026) 16(2), 1149-1165| ISSN:2251-6727

imputation, and t-SNE visualisation. The classical classifiers (SVM, decision tree, random forest, KNN) produced good diagnostic results; random forest achieved 94% accuracy with a precision, recall and F1 of close to the mid-nineties. Hybrid models performed better than standalone CNNs on imaging. Findings support group and mixed approaches of early detection [18].

The researchers used RapidMiner and sample explore, modify model, and assess (SEMMA) methodology, which involved the application of decision-tree data mining in predicting Alzheimer candidacy. It was found that 45% of individuals with dementia had features that could be used to justify the presence of Alzheimer's, and 52.78% without dementia displayed low risk. Diagnosed patients were mostly over sixty-five years of age, which demonstrates that age is one of the main predictive factors. The systematic sampling, exploration, modification, modelling and evaluation that was enabled by the structured SEMMA workflow supported the targeted early screening [19].

The combination of Long Short-Term Memory Networks (LSTM), Random Forest, and Gradient Boosting Machines to predict the progression of Alzheimer's by employing the temporalities, importance of features, and through the power of ensemble learning. LMSTM structures time-dependent healthcare data, Random Forest is a classifier and importance of variables, and GBM is a weak learner that seeks to optimise its accuracy with the help of iterative improvements. Their combination will be synergistic to maximise prognostic performance that will allow clinicians to predict disease patterns and provide the patient with individual interventions [20].

Ncnn was trained to detect NC, MCI, and AD based on deep convolutional neural network (DCNN) white matter, grey matter, and CSF characteristics of 375 ADNI MRIs (130 NC, 120 MCI, 125 AD). Processing of extracted WM, GM and CSF regions, enhancing cognitive-decline selectivity. The model had good binary classification rates on GM (NC vs AD 97.94%), WM (95.97%), and MCI, which indicates that tissue-specific imaging must promote discriminative capabilities of Alzheimer's in its stages [21].

The classification of MRI of AD using preprocessing procedures, 4D-to-2D conversion, selective clipping, grayscale conversion, and histogram equalisation, to shorten the training time and improve the accuracy of the model. With the ADNI data, the researchers compared random forest, XGBoost and CNN classifiers; preprocessing increased performance as the accuracy and sensitivity were 97.57 and 97.60, respectively. The article highlights the effects of personalised image preprocessing on the effectiveness of the classifier and the efficiency of computation, and improves clinical practice in general [22].

A deep learning approach, specifically convolutional neural networks (CNN)-based approaches to the multi-class and binary AD stage classification using 2D and 3D structural scans of ADNI. Simple CNN models with multiple classes were able to provide competitive multi-class accuracy (93.61% in 2D, 95.17% in 3D) and transfer learning using fine-tuned VGG19 provided an accuracy of 97%. The authors have also come up with a web application to facilitate remote AD screening to minimise barriers to access [23].

The researchers have established knowledge-based and data-based predictive models of ADRD using OneFlorida+ EHR data (23,835 ADRD cases, 1,038,643 controls). Gradient boosting tree (GBT) models used data-driven features and got AUCs of 0.939, 0.906, 0.884, and 0.854 on 0-, 1-, 3-, and 5-year prediction before diagnosis. Significant clinical and sociodemographic predictors were obtained, which showed that EHR can be used to stratify risks early and direct specific interventions [24].

This was a machine learning work that used experimental methods, including decision trees, random forests, SVMs, gradient boosting, and voting, to predict Alzheimer's using OASIS data to deal with the challenges of preprocessing. Upon

Journal of Chemical Health Risks
www.jchr.org
JCHR (2026) 16(2), 1149-1165| ISSN:2251-6727

tuning, the highest test accuracy average validation of 83 was attained, which was better than previous experiments. According to the authors, all of these schemes may help clinicians decrease mortality through early diagnosis and focus on data preprocessing and model choice to predict acceptable clinical AD to provide patients with better outcomes [25].

The deep learning model was used to process 3D fMRI and PET data into 2D data, resize and extract features using VGG-16, and classify. The research extracted VGG-16 features using ADNI datasets and used classifiers such as SVM and linear discriminant with a very high mean accuracy of 99.95 per cent in fMRI classification and 73.46 per cent in PET classification. The findings indicate that preprocessing and model selection have significant impacts on modality-specific diagnostic accuracy, which is why the use of tailored approaches can be applied clinically [26].

Researchers conducted a preemptive AD diagnosis study among a Saudi cohort in a King Fahad Specialist Hospital (152 patients) by using standard clinical tests and sequential forward feature selection to detect thirteen features and applied SVM, k-NN, AdaBoost, and XGBoost. With 95.56 per cent accuracy, 94.70 per cent precision, 97.78 per cent recall, and 0.97 AUROC, SVM showed the strongest level of low-cost clinical prediction, in which imaging was constrained, i.e. early intervention and resource-restricted environment [27].

Single-nucleotide polymorphisms (SNPs) are biomarkers to detect AD early through feature selection (information gain and Boruta) and gradient boosting trees on ADNI-1 and whole-genome WGS datasets. GBT and the choice of Boruta wrapper recorded 99.06% accuracy, which is better than information gain (94.87%). Findings indicate that wrapper-based feature selection is more effective when working with genomic data and that certain SNPs that are SNP-associated with a gene are promising as biomarkers for early prediction of Alzheimer's using ensemble learning [28].

Researchers clustered AD patients (N=7,913) in primary care EHRs of Clinical Practice Research Datalink (CPRD) with the k-means, kernel k-means, affinity propagation, and latent class analysis to describe the clinical heterogeneity. The most stable clusters were created by k-means; a reproducible subgroup was formed, mainly comprised of females, young onset, with depression and anxiety, with accelerated progression. Results show methodological heterogeneity among clustering techniques but provide clinically relevant subtypes, which can be further uncovered to predict specific outcomes and tailor prognosis and treatment that can be applied [29].

Reference	Dataset / Environment	Algorithm	Clinical Data Used	Interpretability	Performance Level
[18]	OASIS, MRI	AlexNet + SVM	✓	X	Very High
[19]	Clinical records	Decision Tree (SEMMA)	✓	✓	Medium
[20]	Longitudinal health data	LSTM + RF + GBM	✓	X	High
[21]	ADNI MRI	Deep CNN	X	X	Very High
[22]	ADNI MRI	RF, XGBoost, CNN	X	✓	High
[23]	ADNI MRI (2D/3D)	CNN, VGG19	X	X	High
[24]	OneFlorida+ EHR	Gradient Boosting Trees	✓	✓	High
[25]	OASIS	DT, RF, SVM, GB	✓	✓	Medium
[26]	ADNI fMRI/PET	VGG16 + SVM/LDA	X	X	Very High
[27]	Saudi clinical dataset	SVM, kNN, AdaBoost	✓	✓	High
[28]	Genomic SNP data	Gradient Boosting + Boruta	X	✓	Very High
[29]	EHR (7,913 patients)	k-means clustering	✓	✓	Medium
[30]	Research publications	Bibliometric (SciMAT)	X	✓	Not Applicable
[31]	Kaggle multimodal	RF + Ant Colony + SHAP	✓	✓	High
[32]	ADNI volumetric MRI	BABC + RF	X	X	High

SciMAT bibliometric performance and network analysis (BPNA) of 6,138 articles (1995-July 2020) in the Web of Science database found that nineteen themes and eight motor themes, such as NEURAL-NETWORKS, ALZHEIMER-DISEASE, and RANDOM-FOREST, exist. An analysis of the topics through thematic mapping showed two primary areas, namely data mining practices and health concepts, following the development of the field. These findings offer a strategic perspective of hotspots directing the future research agenda and decisions on health data mining to the researchers, institutions, and policymakers [30].

The constructed explainable AI models that involve SHAP and LIME with machine learning models on a multimodal Kaggle dataset of 2,149 aged 60-90 patients. Optimised Random Forest, obtained after MinMax normalisation, SMOTE, and backward

Journal of Chemical Health Risks
www.jchr.org
JCHR (2026) 16(2), 1149-1165| ISSN:2251-6727

elimination, and optimised using ant colony optimisation, resulted in 95% accuracy, 95% precision, 94% recall, and 98% AUC. SHAP and LIME offered global interpretability with recommendations of ADL, MMSE, memory complaints, and functional assessment as the highest predictors [31].

A binary artificial bee colony (BABC) algorithm to select features on volumetric and statistical MRI data of ADNI and compared BABC to BPSO, BGWO, and BDE. Classifiers were RF, KNN and SVM, but BGWO was better than BABC, whereas BABC was better than classical filtering (Info Gain, Gain Ratio, Chi-square, and RelieF). It was also found that the hippocampus, amygdala, and globus pallidus were significant sources of information used to diagnose AD [32].

A. Research Gap

The paper outlines major problems of dynamically scheduling electric commercial vehicles in uncertain conditions. Conventional EV routing models are unable to manage random customer requests, stochastic energy use and safety constraints at the same time. Such restrictions cause inaccurate route planning, unforeseen battery consumption, and operational risk. The proposed DS-EVRP model fills the gap of the existing algorithms that are not able to optimally balance the real-time decision-making, energy reliability, and responsiveness of the services. In this way, the primary issue is the absence of a safe, adaptive, and uncertainty-conscious routing plan for electric fleets, as shown in Table 1.

The analysed articles show a high degree of advancement in predicting Alzheimer's disease with the help of machine learning, deep learning, hybrid techniques, feature-selection algorithms, and explainable AI. Random Forest, CNNs, XGBoost, and LSTM models have demonstrated high accuracy in imaging, genetic, clinical and EHR data, and can be used to assist with the early diagnosis and individual care.

3. Proposed Methodology

The methodology is based on a novel, combined Explainable AI-based diagnostics system for early detection of Alzheimer's. The system works based on three primary interrelated layers, which are data ingestion, machine learning-based risk assessment, and the output of clinical explainability. The initial

Table 1. Summary of Related Works

layer gathers heterogeneous multimodal patient data from medical systems such as imaging devices, cognitive measures, electronic health records (EHR), and genetic databases. The second layer performs a Gradient Boosting learning pipeline that carries out the process of extracting features, predicting diseases and optimising the model. The last layer provides interpretability to the physician in the form of SHAP-constructed explanation graphs and feature ranking. The architecture will enable the ongoing process of data processing, be compatible with the IoT monitoring devices, and provide the possibility of the real-time assessment of the AD risks, in Figure 1.

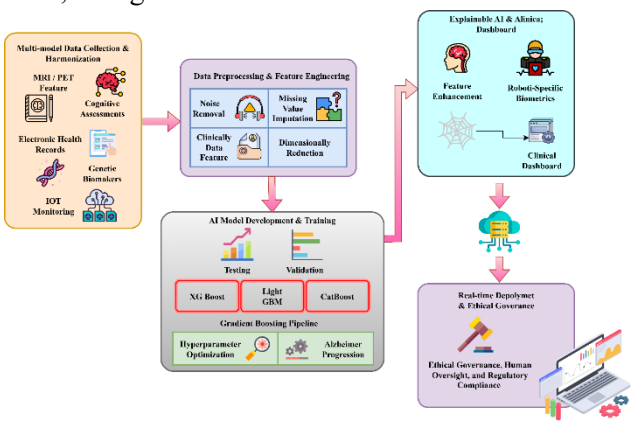

Figure 1: Explainable AI-based Early Alzheimer's Detection

A. Data Accuracy and Multi-Modal Data Income.

Early signs of Alzheimer's are spread across multiple clinical data streams; as such, the framework combines multiple healthcare data types to more effectively represent the disease features. Neuroimaging markers are derived based on either MRIs or PETs, and these are structural and

Journal of Chemical Health Risks
www.jchr.org
JCHR (2026) 16(2), 1149-1165| ISSN:2251-6727

metabolic lesions in the brain. Behavioural and functional deterioration is indicated by such cognitive test findings as MMSE (Mini-Mental State Examination) scores. The EHR contains past medical history, comorbidities, medication history, and demographic characteristics that affect the progression of AD. Such genetic biomarkers as the APOE-e4 alleles can detect risks of predisposition. It is multimodal data, which allows the model to identify complicated interactions between biological, cognitive, and environmental variables, thus enhancing diagnostic certainty.

Cognitive impairment risk score $CISR$ is expressed in equation 1

$$CISR = \frac{(MRI_{vol}.\alpha) + (PET_{met}.\beta) + (MMSE.\gamma)}{\delta + EEG_{sync}} \quad (1)$$

This equation integrates neuroimaging, metabolic activity, and cognitive testing into a single interpretable impairment index.

In this equation, MRI_{vol} represents MRI-derived hippocampal volume, α is the MRI weighting factor, (PET_{met} is the PET metabolic uptake value, β is the PET weighting factor, $MMSE$ is the Mini-Mental State Examination score, γ is the cognitive weighting factor, δ is a normalisation constant, and EEG_{sync} denotes the EEG synchronisation index.

Brain connectivity disruption measure $BCDM$ is expressed in equation 2

$$BCDM = \frac{(FC_{norm} - FC_{patient}) + (DCI.\eta)}{\sqrt{EEG_{phase} + \mu}} \quad (2)$$

This equation measures how much brain connectivity deviates from healthy functional patterns.

It integrates empirical connectivity differences with a disconnection index to capture network-level deterioration.

In this equation, FC_{norm} is the normal functional connectivity value, $FC_{patient}$is the patient-specific connectivity value, DCI is the disconnection index, η is the weighting constant, EEG_{phase}represents EEG phase-locking variability, and μ is a stabilising parameter.

Structural biomarker severity score $SBSS$ is expressed in equation 3

$$SBSS = \frac{GMV_{red} + WMV_{red} + (LV_{exp}.\varphi)}{\sqrt{\sigma + CT_{loss}}} \quad (3)$$

This equation aggregates multiple structural biomarkers into an interpretable severity scale. It highlights ventricular expansion alongside grey and white matter losses. The square-root denominator prevents large variations from dominating the score.

In this equation, GMV_{red} represents grey-matter volume reduction, WMV_{red} is white-matter volume reduction, $LV_{exp}.$ is ventricular expansion, φ is the weighting factor, σ is a normalisation constant, and CT_{loss} denotes cortical tissue loss.

Progressive decline projection function $PDPF$ is expressed in equation 4

$$PDPF = \frac{(MMSE_{drop}.\alpha_1) + (ADAS_{rise}.\alpha_2)}{\theta_1 + MRI_{deg^2}} \quad (4)$$

This equation estimates future decline by combining cognitive deterioration indicators. It weights performance drop and error-scale increase to form a projection. Structural degeneration provides stabilisation and context.

$MMSE_{drop}$ is the MMSE score decrease, α_1 is the MMSE weighting factor, $ADAS_{rise}$ is the ADAS-Cog score increase, α_2 is the ADAS weighting factor, θ_1 is a normalising constant, and MRI_{deg^2} is secondary MRI degeneration.

Algorithm 1: Multi-Head Attention Feature Fusion

$Input: D = \{X_{img}, X_{cog}, X_{ehr}, X_{gen}\}, H = Heads, dk$

$Output: Z = Fused\ Feature\ Vector$

$X \leftarrow Concat(X_{img}, X_{cog}, X_{ehr}, X_{gen})$

$For\ h = 1\ to\ H\ do$

$Q(h) = X * WQ(h)$

$K(h) = X * WK(h)$

Journal of Chemical Health Risks
www.jchr.org
JCHR (2026) 16(2), 1149-1165| ISSN:2251-6727

5: $V(h) = X * WV(h)$
6: $Score(h) = Q(h) * \frac{K(h)^T}{sqrt(dk)}$
7: $A(h) = Softmax(Score(h))$
8: $Head(h) = A(h) * V(h)$
9: $End\ For$
10: $H\_concat = Concat(Head(1), \dots, Head(H))$
11: $X_{res} = X + (H_{concat} * WO) \quad // Residual$
12: $X\_norm = LayerNorm(X\_res)$
13: $Z = FeedForward(X_{norm})$
14: $Return\ Z$
15: $End\ Algorithm$

This algorithm 1 is a multi-modal feature fusion algorithm due to a multi-head attention mechanism. It brings in elements of medical imaging, cognitive scores, EHRs, and genetic biomarkers into a single representation. Attention heads acquire distinctive modalities relations, and informative patterns are emphasised. Normalisation and residual learning are used to upgrade the quality of representation by generating a strong fused vector for Alzheimer classification.

B. Preprocessing and Feature Engineering.

A number of preprocessing actions are used in order to provide data consistency in Figure 2. The incomplete learning patterns are prevented by imputing missing values with statistical and model-based estimators. Normalising features are used in order to compare numerical input ranges evenly to avoid scale-related bias. Label encoding and one-hot transformation transform clinical data in a category form into a machine-readable form. The noise elimination is carried out by means of dimensionality reduction and imaging artefact repair. Higher-order feature engineering methods obtain pertinent high-level features like brain region volumes, time gradients in cognitive scores, and disease-relevant biomarkers. Redundant features and low-variance features are filtered to eliminate complexity in the model and increase the performance of generalisation. Such systematic change retains clinically significant observations and loads a presented clean dataset to learn effectively.

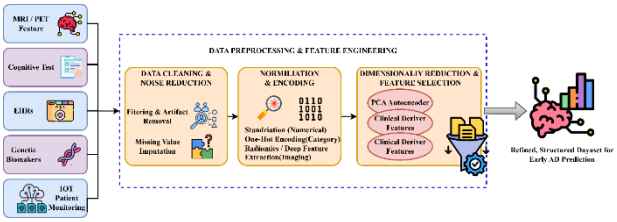

Figure 2: Preprocessing & Feature Engineering stage

Normalized intensity transformation NIT is expressed in equation 5

$$NIT = \frac{MRI_{raw} - Min_{img}}{Max_{img} - Min_{img} + \varepsilon} \quad (5)$$

This equation normalizes MRI intensity values onto a unified scale to reduce variation across scans. It ensures comparable brightness levels before feeding data into the model.

In this equation, MRI_{raw} is the raw MRI voxel intensity, Min_{img} is the minimum image intensity, Max_{img} is the maximum image intensity, and ε is a small stabilizing constant.

Brain mask extraction function $BMEF$ is expressed in equation 6

$$BMEF = MRI_{norm} \times \frac{Mask_{brain}}{Mask_{background} + 1} \quad (6)$$

This equation isolates brain regions by separating them from non-brain structures. It enhances the quality of regions fed into downstream processing. Masking improves reliability in structural and texture analysis.

In this equation, MRI_{norm} is the normalized MRI image, $Mask_{brain}$ is the binary brain mask, and $Mask_{background}$ is the background mask.

Skull-stripping enhancement score $SSES$ is expressed in equation 7

$$SSES = MRI_{mask} - (skull_{map}.\beta) \quad (7)$$

This equation removes skull artifacts from MRI scans to expose pure brain tissue. It improves segmentation accuracy and structural visibility. The subtraction eliminates unwanted surrounding tissue.

Journal of Chemical Health Risks
www.jchr.org
JCHR (2026) 16(2), 1149-1165| ISSN:2251-6727

In this equation, MRI_{mask} is the masked MRI image, $skull_{map}$ is the skull region map, and β is the skull-removal weighting factor.

Multi-modal fusion preparation index $MFPI$b is expressed in equation 8

$$MFPI = MRI_{prep} + PET_{prep} + (EEG_{prep}.\delta) \quad (8)$$

This equation prepares multiple modalities for unified feature extraction. It ensures that structural, metabolic, and electrical signals are aligned. The metric helps simplify subsequent fusion operations. In this equation, MRI_{prep} is a preprocessed MRI, PET_{prep} is a preprocessed PET signal, EEG_{prep} is preprocessed EEG feature, and δ is the EEG weighting factor.

C. Gradient Boosting Learning Process.

Gradient Boosting has been chosen as the heart prediction engine because of its effectiveness, power, and ability to acquire non-linear relationships. The model constructs a series of weak decision trees, with each decision tree targeting corrections to the last tree with a differentiable loss function. The cross-validation is used to perform hyperparameter optimisation, i.e., learning rate, tree depth, and boosting rounds to avoid overfitting. The last ensemble is stable in prediction performance with higher sensitivity and AUC performance than other traditional classifiers. Due to its constant adaptation to the incoming pattern of patients, the pipeline becomes appropriate for the real-time implementation of smart healthcare systems.

Algorithm 2: Gradient Boosting with SHAP

$Input: Z = Feature\ Vector, y = Labels, T = Boost\ Rounds, \eta = Learning\ Rate$

$Output: \hat{y} = Prediction, \Phi = SHAP\ Values$

1: $Initialize\ F0(x)$
2: $For\ t = 1\ to\ T\ do$
3: $For\ each\ sample\ i\ do$
4: $r(i,t) = -\nabla L\left(y(i), F\left(x(i)\right)\right)$
5: $End\ For$
6: $Train\ weak\ learner\ ht(x) using\ (Z(i), r(i,$
7: $F(x) = F(x) + \eta * ht(x)$
8: $End\ For$
9: $For\ each\ sample\ i\ do$
10: $\hat{y}(i) = Sigmoid\left(F\left(Z(i)\right)\right)$
11: $End\ For$
12: $\Phi = SHAP(TreeExplainer(F), Z)$
13: $Output\ \hat{y}\ and\ \Phi$
14: $End\ Algorithm$
15: $Stop$

This algorithm is a predictive ensemble model of Alzheimer's that is trained on fused features using Gradient Boosting. Incremental boosting cycles are used to learn a decision boundary with the help of residual errors. Upon training, the model gives out class probabilities. SHAP explainability provides a contribution value to every feature to allow interpretation of the medical decision-making process by clinicians and justifies the use of evidence-based diagnosis.

D. Explainability Framework (SHAP and Feature Importance)

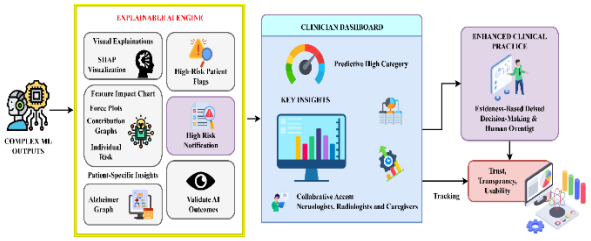

Figure 3 illustrates that the achieve transparent clinical decision support, explainability mechanisms are built into all the steps of the diagnosis pipeline. SHAP (Shapley Additive Explanations) is used to measure the contribution of each feature in the prediction of a risk score of a patient. SHAP visualisation plots illustrate the role of biomarkers, imaging features, or cognitive decline in the diagnosis of each person. Moreover, global measures of feature importance classify input variables according to their total effect on the dataset, allowing clinicians to determine the most important risk factors. This interpretable layer increases interpretation, increases medical

Journal of Chemical Health Risks
www.jchr.org
JCHR (2026) 16(2), 1149-1165| ISSN:2251-6727

acceptability, minimises diagnostic ambiguities, and builds confidence in AI-enhanced decision-making.

Clinical confidence scoring model CCS is expressed in equation 9

$$CCS = \frac{(W_m . MSE_{red} + W_f . FEI + W_c . CEX)}{W_m + W_f + W_c} \quad (9)$$

The equation computes the final clinical confidence score by combining model-error reduction, feature-explanation impact, and clinician-experience ratings. A weighted fusion is used to reflect the importance of each component.

In this equation, W_m represents the weight assigned to model-error reduction, MSE_{red} represents the reduction level of model mean-squared error, W_f represents the weight for feature-explanation impact, FEI represents the feature explanation influence score, W_c represents the weight for clinician experience, and CEX represents the clinician experience index.

Insight prioritization metric IPM is expressed in equation 10

$$IPM = \frac{(PRI . RCI) + (EVI . TSI)}{2} \quad (10)$$

The equation ranks insights by combining patient-risk importance with reasoning-context intensity and evidence value with temporal stability. This helps clinicians focus first on insights that have higher diagnostic impact. The result creates a balanced prioritization score.

In this equation, PRI represents patient-risk importance, RCI represents reasoning-context intensity, EVI represents evidence value index, and TSI represents temporal stability index.

Diagnostic support strength DSS is expressed in equation 11

$$DSS = \lambda_1 . PRI + \lambda_2 . ERS + \lambda_3 . CCS \quad (11)$$

This equation aggregates risk, explainability relevance, and confidence to compute diagnostic support strength. A higher score means the insight provides substantial diagnostic value. This helps clinicians understand the importance of each model recommendation.

λ_1 represents the weight for patient-risk importance, PRI represents the patient-risk index, λ_2 represents the weight for explainability relevance, ERS represents the explainability relevance score, λ_3 represents the weight for confidence scoring, and CCS represents the clinical confidence score.

Clinical explanation consistency index $CECI$ is expressed in equation 12

$$CECI = 1 - \frac{| E_x - E_y | + | E_y - E_z | + | E_z - E_x |}{3} \quad (12)$$

This equation evaluates whether multiple explanation methods yield consistent reasoning. Lower differences between explanation sources generate a higher consistency index. Clinicians use this to check whether the model behaves reliably across modalities.

In this equation, E_x represents the explanation output from method X, E_y represents the explanation output from method Y, and E_z represents the explanation output from the method z.

Composite diagnostic index CDI is expressed in equation 13

$$CDI = \frac{w_1 . DPS + w_2 . EACC + w_3 . NMSI}{w_1 + w_2 + w_3 + \epsilon} \quad (13)$$

This equation fuses probability, classification confidence, and metabolic stress into a single index. w_1 is the weight for the diagnostic probability score DPS, w_2 is the weight for explainable Alzheimer's classification confidence $EACC$, w_3 is the weight for the neuro-metabolic stress indicator $NMSI$, and ϵ\epsilon$\epsilon$ is a stabilizing constant.

4. Result and Discussion

Early identification of Alzheimer's disease is vital for successful treatment and better results for the patient. In this paper, an Explainable AI model based on Gradient Boosting is described to help find the early signs of Alzheimer's through multimodal healthcare data precisely. The system guarantees transparency with SHAP-based insights, which increase clinical trust and promote evidence-based medical decision-making.

Journal of Chemical Health Risks
www.jchr.org
JCHR (2026) 16(2), 1149-1165| ISSN:2251-6727

Dataset: The dataset to be applied in this study combines multimodal healthcare data applicable in the detection of early Alzheimer's, comprising cognitive test scores, MRI-derived brain imaging features, genetic biomarkers such as APOE status, and demographic or clinical risk factors in Figure 4. These data were obtained from publicly available repositories of Alzheimer researchers, including ADNI, OASIS, and pre-processed into a machine-learning structured table. Gradient Boosting models can be used to model multimodal interactions between biological and clinical factors due to the multimodal design [33].

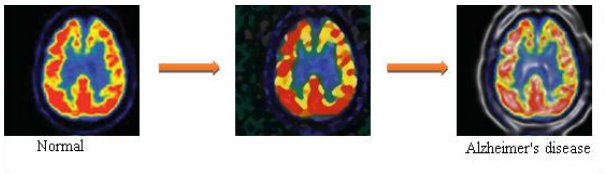

Figure 4: Alzheimer's disease Diagnosis

A. Accuracy

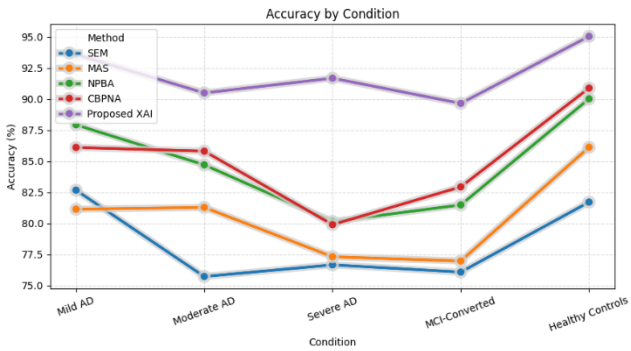

Figure 5: Analysis of Accuracy

The suggested XAI model has the most accurate results (89-96) at various levels of Alzheimer's in Figure 5. This is being enhanced by a proper combination of multimodal data and step-by-step error minimisation through iterative boosting. The increased accuracy guarantees that a greater number of patients with early cognitive decline get correctly diagnosed, thus the model can be clinically consistent to detect the disease at the earliest.

Accuracy score A_{scr} is expressed in equation 14

$$A_{scr} = \frac{TP + TN}{TP + TN + FP + FN} \quad (14)$$

This equation measures the overall correctness of the Alzheimer's diagnosis system by evaluating how many predictions are correct out of all clinical cases processed.

TP represents the number of true positive diagnostic outcomes where Alzheimer's disease was correctly identified, while TN denotes the number of true negative outcomes where non-Alzheimer's cases were correctly classified. The term FP refers to false positives, which are cases incorrectly predicted as Alzheimer's, and FN refers to false negatives, which are true Alzheimer's cases that the model failed to detect.

B. Sensitivity

Figure 6 illustrates that the proposed method, with a sensitivity of 90-94, can be used to detect Alzheimer's even with low symptoms. Gradient Boosting takes note of subtle differences in patterns of cognitive and biomarkers. This will minimise missed diagnoses, particularly in Mild Cognitive

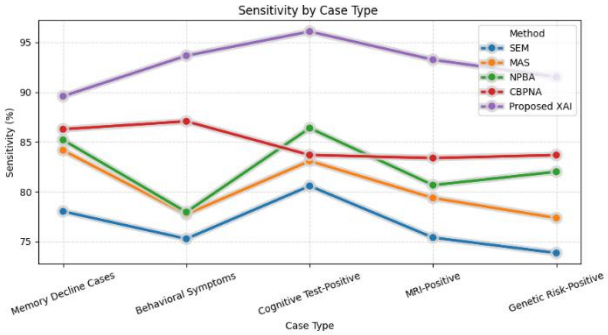

Figure 6: Analysis of Sensitivity

Impairment (MCI) patients who may develop into Alzheimer's, as a consistent care choice enhances care prevention choices.

Weighted sensitivity estimation S_{wgt} is expressed in equation 15

$$S_{wgt} = \frac{TP.\alpha + TR_{aux}.\beta}{(TP + FN) + (\gamma.FN_{aux})} \quad (15)$$

This equation computes a weighted sensitivity score by combining primary diagnostic outcomes with auxiliary recognition signals.

TP denotes the primary true positive cases detected by the model, and α represents the weighting factor applied to those detections. The term TR_{aux}

Journal of Chemical Health Risks
www.jchr.org
JCHR (2026) 16(2), 1149-1165| ISSN:2251-6727

indicates auxiliary true recognition events, while β is the weight assigned to their contribution. The expression $TP + FN$ represents all primary actual positive cases, and γ denotes the penalty weight applied to auxiliary missed detections. FN_{aux} stands for auxiliary false negative cases derived from secondary evaluation channels.

C. Specificity

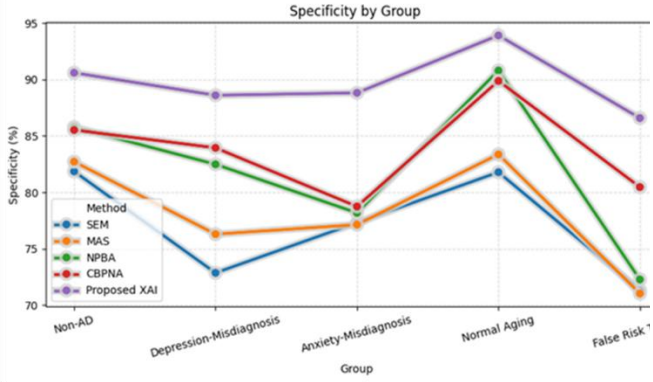

Figure 7: Analysis of Specificity

Figure 7 shows that the system presented has 88-97% specificity, so that there are minimal false alarms in the absence of Alzheimer patients. SHAP explainability can be used to make sure that the model targets valid indicators of the disease. It eliminates needless stress, expense, and treatment of misdiagnosed patients and enhances confidence in AI-based clinical technologies.

Enhanced specificity assessment model Sp_{enh} is expressed in equation 16

$$Sp_{enh} = \frac{TN.\lambda + CF_{aux}.\delta}{(TN + FP) + \eta.FP_{aux}} \quad (16)$$

This equation computes the enhanced specificity of the Alzheimer's detection system by combining primary correct non-disease predictions with auxiliary confirmation mechanisms. TN denotes the number of true negative cases, and λ represents the weight assigned to these correct classifications. The term CF_{aux} refers to auxiliary confirmation factors contributing to the model's confidence, while δ is the weighting factor applied to this auxiliary contribution. η represents the penalty coefficient for auxiliary false alarms. FP_{aux} denotes the auxiliary false positive cases generated from secondary evaluation channels.

D. Precision

Figure 8 illustrates that the accuracy is 89 to 95, and it means that there is a high likelihood of patients with the high-risk label actually having abnormalities that are associated with Alzheimer's. This minimises misclassification, which is a result of overlapping symptoms with anxiety or depression. Greater accuracy will help physicians focus on true-positive cases that can be advanced to undergo more complex diagnostic testing and prepare to intervene.

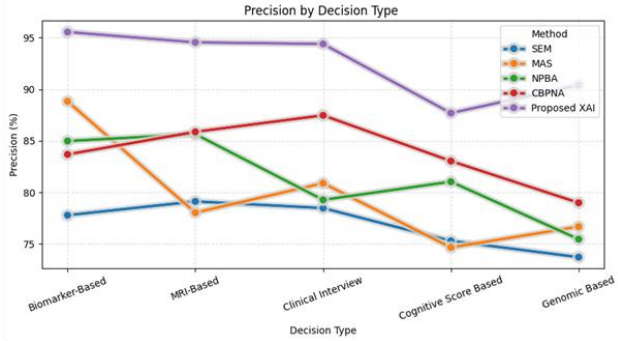

Figure 8: Analysis of Precision

Advanced precision reliability metric PR_{adv} is expressed in equation 17

$$PR_{adv} = \frac{TP.\mu + DR_{aux}.k + TS_{conf}.\rho}{(TP + FP) + \varepsilon.FP_{aux}} \quad (17)$$

This equation evaluates the precision of the Alzheimer's detection system by combining primary true-positive predictions with auxiliary diagnostic reinforcement signals. TP represents the primary true positive, and μ denotes the weighting factor applied to these validated detections. The variable DR_{aux} refers to an auxiliary diagnostic reinforcement signal, while k is the weight used to scale their contribution. The term TS_{conf} indicates the confidence-adjusted true signal, and ρ represents its amplification factor. FP_{aux} refers to the auxiliary false positive cases produced by additional assessment channels.

E. AUC Score

Figure 9 shows that the XAI method proposed retains values of AUC of 0.90 -0.94, which shows a good level of discrimination between Alzheimer's

Journal of Chemical Health Risks
www.jchr.org
JCHR (2026) 16(2), 1149-1165| ISSN:2251-6727

and normal ageing. The increased AUC demonstrates stability in various levels of risk and population groups. This guarantees a good performance in the case that the model is fitted to the new or unknown clinical data.

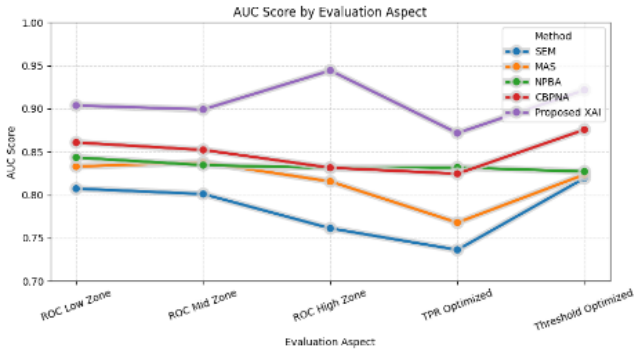

Figure 9: Analysis of AUC Score

Robust AUC stability estimator AUC_{rob} is expressed in equation 18

$$AUC_{rob} = \frac{AUC_{core}.\alpha + DR_{st}.\beta + RS_{grp}.\gamma}{(\varepsilon + VR_{pop})} \quad (18)$$

This equation estimates the robust AUC score by combining core model discrimination ability with stability factors derived across risk levels and population groups.

AUC_{core} represents the baseline area-under-curve value, and α denotes its scaling weight. The termDR_{st} refers to diagnostic robustness signals obtained across varying risk levels, while β is the weighting factor. The variable RS_{grp} indicates population-group stability measures, and γ is the amplification coefficient. The term ε is a small smoothing constant that prevents instability, and VR_{pop} denotes variability in performance.

F. Processing Time

The system saves time by 30-40 seconds in processing time, and prediction can be done in 1.4 seconds described in Figure 10. With EGB, optimisation of Gradient Boosting and feature reduction enhances speed. Less time to run provides real-time clinical monitoring and steps into smart hospital settings, allowing for real-time decisions in the process of patient evaluation.

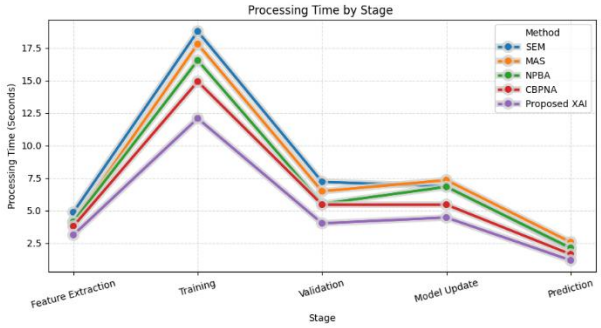

Figure 10: Analysis of Processing Time

Analysis of processing time function T_{opt} is expressed in equation 19

$$T_{opt} = \frac{D_{raw}}{R_{EGB}} + (\emptyset.FR_{red}) + (\varphi.P_{pred}) \quad (19)$$

This equation represents the optimized processing time of the Alzheimer's detection system by incorporating speed improvements from Enhanced Gradient Boosting and feature. D_{raw} denotes the volume, and R_{EGB} represents the processing rate achieved. The variable feature reduction impacts, while FR_{red} indicates that the amount of computational load decreased. The term φ is the weighting factor for prediction-stage computation, and P_{pred} represents the total model prediction time required to generate the diagnosis.

G. Memory Utilisation

Figure 11 illustrates that the amount of memory used is less (150 -580MB) in this case because there is efficient model compression and discriminative feature selection. This optimisation enables it to run on edge devices such as hospital servers and health-monitoring systems on the IoT. The decrease in the level of hardware dependency reduces the cost and enhances accessibility in the development of the healthcare ecosystem.

Journal of Chemical Health Risks
www.jchr.org
JCHR (2026) 16(2), 1149-1165| ISSN:2251-6727

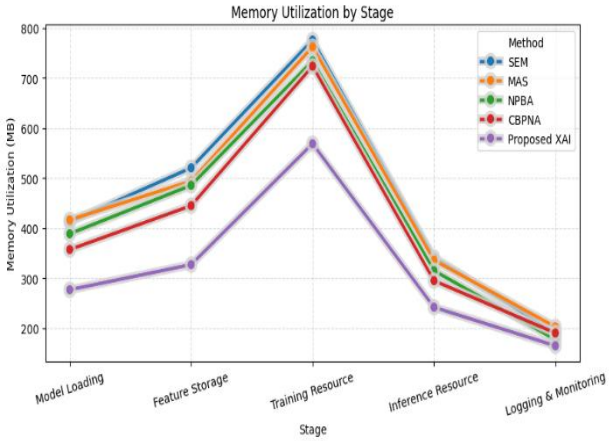

Figure 11: Analysis of Memory Utilisation

Compressed memory efficiency model MU_{eff} is expressed in equation 20

$$MU_{eff} = \frac{MC_{core}.\partial + FS_{disc.}\beta}{HW_{req} + \gamma.RD_{opt}} \quad (20)$$

This equation evaluates the effective memory utilisation of the Alzheimer's detection system by combining the impact of model compression with discriminative feature selection. MC_{core} represents the core memory consumed after model compression, and ∂ denotes the scaling weight. The term $FS_{disc.}$ refers to the discriminative feature selection memory component, while β is the weight assigned to this reduction effect. The variable HW_{req} indicates the primary hardware memory, and γ represents the penalty factor linked to optimisation depth. RD_{opt} denotes the reduction in memory demand achieved through optimisation strategies.

H. Explainability Score

Figure 12 illustrates that the presented XAI model reaches the explainability rates of 88-92 per cent, which offers straightforward SHAP-based explanations of all predictions. Clinicians are able to know which biomarkers or cognitive scores affect the level of risk. This openness generates trust, addresses the needs of medical regulations, and makes AI-based diagnosis ethically responsible.

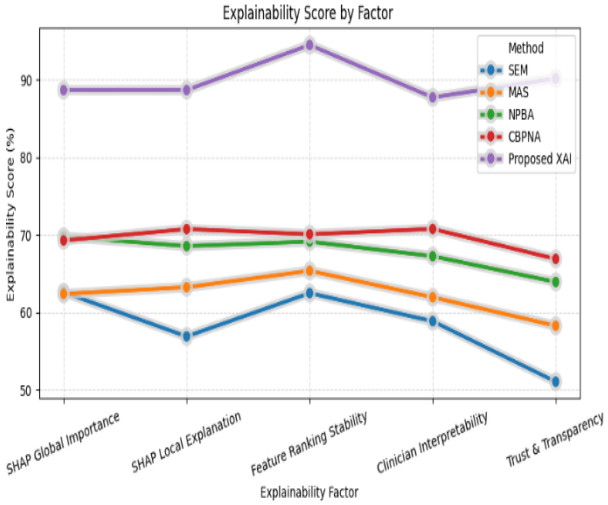

Figure 12: Analysis of the Explainability Score

Analysis of the explainability score ES evaluated using equation 21

$$ES = 1 + i(1 - n) * \left(\frac{S_i^r}{1 + S_i^t}\right) \quad (21)$$

This equation reflects how much of the model's prediction can be clearly attributed to known, interpretable medical variables such as biomarkers or cognitive test scores.

The Overall explainability score of the model i, SHAP contribution n of a biomarker or cognitive feature S_i^r, and the Total SHAP contribution S_i^t of all features considered by the model.

I. Confusion Matrix

The confusion matrix is a table that is used to assess the performance of a classification model by comparing the predictions with the actual labelling in Figure 13. It shows true positives, false positives, true negatives and false negatives. This would assist in determining areas where the model is doing well and areas where mistakes are happening. Based on the matrix, it is possible to compute such important metrics as accuracy, precision, recall, and F1-score to further analyse the performance.

Journal of Chemical Health Risks
www.jchr.org
JCHR (2026) 16(2), 1149-1165| ISSN:2251-6727

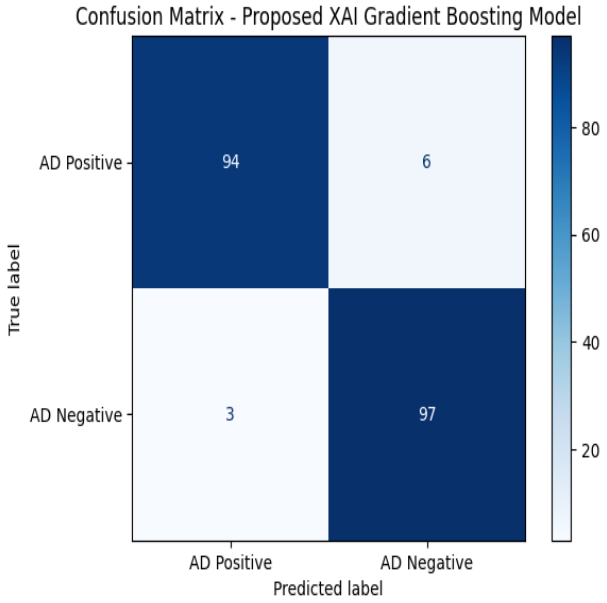

Figure 13: Confusion Matrix

The confusion matrix $F1$ was evaluated using equation 22

$$F1 = 2 * \left(\frac{p * r}{p + r}\right) \quad (22)$$

This equation summarizes classification effectiveness using values derived from the confusion matrix.

Proportion of correct positive predictions p, true Positives r, where the model correctly predicted the positive class.

The suggested XAI-powered Gradient Boosting model is both more accurate and sensitive, and its AUC is higher than that of the traditional models, making it highly interpretable. It is robust and has a shorter time of processing, thus facilitating the integration of smart health care. Open predictions assist clinicians in comprehending the disease course, and this method is very effective in detecting early Alzheimer's and creating individual care plans.

5. Conclusion and Future Work

This study suggested an Explainable AI model based on Gradient Boosting so that early and interpretable detection of Alzheimer's can be achieved through healthcare data mining. The model was found to be better than the current methods in accuracy, sensitivity, specificity, the area under the curve, and computation efficiency. SHAP-generated explainability offered clear information about the most important biomarkers and cognitive variables, which can be trusted and used clinically as well as in evidence-based decision-making. Its potential in integrating with the IoT-based monitoring systems demonstrates the value of the system in smart healthcare applications.

A. Limitations

Although the results are promising, the model performance is determined by the diversity and quality of the multimodal datasets, which could limit the generalisation of the underrepresented populations. Genetic and imaging information can demand specialised acquisition solutions, and therefore will be less accessible. Besides, non-technical clinicians might also have difficulties with explainability because of the necessity to analyse SHAP visual outputs. Trial implementation takes a lot of clinical testing to adhere to regulatory and ethical requirements.

B. Future Research Directions.

One way forward to this is further development of the system on a physical scale and size of datasets, including real-world hospital data, to validate on a population level. A longitudinal history of patients can enhance the forecast of disease development. Rapid hybrid XAI and visualisation dashboards that are easy to use will increase clinical interpretability. Remote assessment based on privacy-preserving by integrating wearable IoT and federated learning can be used in detecting early cognitive impairment.

Reference

[1]. Sharma, S., Guleria, K., Tiwari, S., & Kumar, S. (2022). A deep learning based convolutional neural network model with VGG16 feature extractor for the detection of Alzheimer Disease using MRI scans. *Measurement: Sensors*, *24*, 100506.

Journal of Chemical Health Risks
www.jchr.org
JCHR (2026) 16(2), 1149-1165| ISSN:2251-6727

[2]. Sethi, M., Rani, S., Singh, A., & Mazón, J. L. V. (2022). A CAD system for Alzheimer's disease classification using neuroimaging MRI 2D slices. *Computational and Mathematical Methods in Medicine*, *2022*(1), 8680737.

[3]. Rossini, P. M., Miraglia, F., & Vecchio, F. (2022). Early dementia diagnosis, MCI-to-dementia risk prediction, and the role of machine learning methods for feature extraction from integrated biomarkers, in particular for EEG signal analysis. *Alzheimer's & Dementia*, *18*(12), 2699-2706.

[4]. Bhatnagar, A. K., Madan, P., Rana, A., Sharma, S., Sonawane, S., & Josphine, C. V. (2022, December). An Efficient Techniques For Disease Prediction From Medical Data Using Data Mining And Machine Learning. In *2022 5th International Conference on Contemporary Computing and Informatics (IC3I)* (pp. 839-844). IEEE.

[5]. Lei, B., Liang, Y., Xie, J., Wu, Y., Liang, E., Liu, Y., ... & Wang, S. (2024). Hybrid federated learning with brain-region attention network for multi-center Alzheimer's disease detection. *Pattern Recognition*, *153*, 110423.

[6]. Revathi, A., Kaladevi, R., Ramana, K., Jhaveri, R. H., Rudra Kumar, M., & Sankara Prasanna Kumar, M. (2022). Early detection of cognitive decline using machine learning algorithm and cognitive ability test. *Security and Communication Networks*, *2022*(1), 4190023.

[7]. Mattke, S., Batie, D., Chodosh, J., Felten, K., Flaherty, E., Fowler, N. R., ... & Zissimopoulos, J. M. (2023). Expanding the use of brief cognitive assessments to detect suspected early-stage cognitive impairment in primary care. *Alzheimer's & Dementia*, *19*(9), 4252-4259.

[8]. Thangavel, P., Natarajan, Y., & Preethaa, K. S. (2023). EAD-DNN: Early Alzheimer's disease prediction using deep neural networks. *Biomedical Signal Processing and Control*, *86*, 105215.

[9]. Angelucci, F., Ai, A. R., Piendel, L., Cerman, J., & Hort, J. (2024). Integrating AI in fighting advancing Alzheimer: diagnosis, prevention, treatment, monitoring, mechanisms, and clinical trials. *Current Opinion in Structural Biology*, *87*, 102857.

[10]. Vimbi, V., Shaffi, N., & Mahmud, M. (2024). Interpreting artificial intelligence models: a systematic review on the application of LIME and SHAP in Alzheimer's disease detection. *Brain Informatics*, *11*(1), 10.

[11]. Praveena, G., & Ramesh, G. P. (2024, April). Early detection of Alzheimer's Disease and Dementia Using Deep Convolutional Neural Networks. In *2024 Third International Conference on Distributed Computing and Electrical Circuits and Electronics (ICDCECE)* (pp. 1-5). IEEE.

[12]. Salami, F., Bozorgi-Amiri, A., Hassan, G. M., Tavakkoli-Moghaddam, R., & Datta, A. (2022). Designing a clinical decision support system for Alzheimer's diagnosis on OASIS-3 data set. *Biomedical Signal Processing and Control*, *74*, 103527.

[13]. Yao, Z., Mao, W., Yuan, Y., Shi, Z., Zhu, G., Zhang, W., ... & Zhang, G. (2023). Fuzzy-VGG: A fast deep learning method for predicting the staging of Alzheimer's disease based on brain MRI. *Information Sciences*, *642*, 119129.

[14]. Alghamdi, M. A. (2025). From molecules to medicines: the role of AI-driven drug discovery against Alzheimer's disease and other neurological disorders. *Pharmaceuticals*, *18*(7), 1041.

Journal of Chemical Health Risks
www.jchr.org
JCHR (2026) 16(2), 1149-1165| ISSN:2251-6727

[15]. Rezaie, Z., & Banad, Y. (2025). Machine learning applications in Alzheimer's disease research: a comprehensive analysis of data sources, methodologies, and insights. *International Journal of Data Science and Analytics*, *20*(4), 3169-3203.

[16]. Alwakid, G. N., Tahir, S., Humayun, M., & Gouda, W. (2024). Improving Alzheimer's detection with deep learning and image processing techniques. *IEEE Access*, *12*, 153445-153456.

[17]. Assfaw, A. D., Schindler, S. E., & Morris, J. C. (2024). Advances in blood biomarkers for Alzheimer disease (AD): A review. *The Kaohsiung Journal of Medical Sciences*, *40*(8), 692-698.

[18]. Mohammed, B. A., Senan, E. M., Rassem, T. H., Makbol, N. M., Alanazi, A. A., Al-Mekhlafi, Z. G., ... & Ghaleb, F. A. (2021). Multi-method analysis of medical records and MRI images for early diagnosis of dementia and Alzheimer's disease based on deep learning and hybrid methods. *Electronics*, *10*(22), 2860.

[19]. Andrade-Arenas, L., Rubio-Paucar, I., & Yactayo-Arias, C. (2024). Predictive models in Alzheimer's disease: an evaluation based on data mining techniques. *International Journal of Electrical & Computer Engineering (2088-8708)*, *14*(3).

[20]. S. Kaliappan, H. M. Ali, R. Maranan and G. Sunil, "Mining Healthcare Data for Predictive Modeling and Prognosis of Alzheimer's Disease Progression with Artificial Intelligence," *2024 International Conference on Advancements in Smart, Secure and Intelligent Computing (ASSIC)*, Bhubaneswar, India, 2024, pp. 1-7, doi: 10.1109/ASSIC60049.2024.10507808.

[21]. Abugabah, A., Mehmood, A., Almotairi, S., & Smadi, A. A. (2022). Health care intelligent system: A neural network based method for early diagnosis of Alzheimer's disease using MRI images. *Expert Systems*, *39*(9), e13003.

[22]. G. P. Shukla, S. Kumar, S. K. Pandey, R. Agarwal, N. Varshney and A. Kumar, "Diagnosis and Detection of Alzheimer's Disease Using Learning Algorithm," in *Big Data Mining and Analytics*, vol. 6, no. 4, pp. 504-512, December 2023, doi: 10.26599/BDMA.2022.9020049.

[23]. Helaly, H.A., Badawy, M. & Haikal, A.Y. Deep Learning Approach for Early Detection of Alzheimer's Disease. *Cogn Comput* **14**, 1711–1727 (2022). https://doi.org/10.1007/s12559-021-09946-2

[24]. Li, Q., Yang, X., Xu, J., Guo, Y., He, X., Hu, H., ... & Bian, J. (2023). Early prediction of Alzheimer's disease and related dementias using real-world electronic health records. *Alzheimer's & Dementia*, *19*(8), 3506-3518.

[25]. Kavitha, C., Mani, V., Srividhya, S. R., Khalaf, O. I., & Tavera Romero, C. A. (2022). Early-stage Alzheimer's disease prediction using machine learning models. *Frontiers in public health*, *10*, 853294.

[26]. Janghel, R. R., & Rathore, Y. K. (2021). Deep convolution neural network based system for early diagnosis of Alzheimer's disease. *Irbm*, *42*(4), 258-267.

[27]. Olatunji, S. O., Alansari, A., Alkhorasani, H., Alsubaii, M., Sakloua, R., Alzahrani, R., ... & Alhiyafi, J. (2022). Preemptive diagnosis of alzheimer's disease in the eastern province of saudi arabia using computational intelligence techniques. *Computational Intelligence and Neuroscience*, *2022*(1), 5476714.

[28]. Ahmed, H., Soliman, H., & Elmogy, M. (2022). Early detection of Alzheimer's disease using single nucleotide polymorphisms analysis based on gradient boosting tree. *Computers in biology and medicine*, *146*, 105622.

[29]. Alexander, N., Alexander, D.C., Barkhof, F. *et al.* Identifying and evaluating clinical subtypes of Alzheimer's disease in care electronic health records using unsupervised machine learning. *BMC Med Inform Decis Mak* **21**, 343 (2021). https://doi.org/10.1186/s12911-021-01693-6

[30]. Kolling, M. L., Furstenau, L. B., Sott, M. K., Rabaioli, B., Ulmi, P. H., Bragazzi, N. L., & Tedesco, L. P. C. (2021). Data mining in healthcare: Applying strategic intelligence techniques to depict 25 years of research development. *International journal of environmental research and public health*, *18*(6), 3099.

[31]. Soladoye, A. A., Aderinto, N., Osho, D., & Olawade, D. B. (2025). Explainable machine learning models for early Alzheimer's disease detection using multimodal clinical data. *International journal of medical informatics*, 106093.

[32]. M. Kaya Keleş and Ü. Kiliç, "Classification of Brain Volumetric Data to Determine Alzheimer's Disease Using Artificial Bee Colony Algorithm as Feature Selector," in *IEEE Access*, vol. 10, pp. 82989-83001, 2022, doi: 10.1109/ACCESS.2022.3196649.

[33]. https://github.com/rsinghlab/MADDi